Research Square

Preprints are preliminary reports that have not undergone peer review. They should not be considered conclusive, used to inform clinical practice, or referenced by the media as validated information.

Realization of decoherence-induced average symmetry-protected topological phases on quantum processors

Ruizhe Shen

e0554228@u.nus.edu

National University of Singapore https://orcid.org/0000-0002-6992-9219

Xuejia Yu

Eastern Institute of Technology, Ningbo https://orcid.org/0000-0002-1935-1463

Ching Hua Lee

National University of Singapore https://orcid.org/0000-0003-0690-3238

Article

Keywords:

Posted Date: October 22nd, 2026

DOI: https://doi.org/10.21203/rs.3.rs-11344157/v1

License: This work is licensed under a Creative Commons Attribution 4.0 International License. Read Full License

Additional Declarations: There is **NO** Competing Interest.

Realization of decoherence-induced average symmetry-protected topological phases on quantum processors

Ruizhe Shen,[1,*] Xue-Jia Yu,[2,†] and Ching Hua Lee[1,‡]

[1] *Department of Physics, National University of Singapore, Singapore 117551*
[2] *Eastern Institute of Technology, Ningbo 315200, China*

(Dated: October 14, 2026)

Symmetry-protected topological (SPT) phases are conventionally formulated for pure states protected by exact symmetries. In open quantum systems, however, decoherence generates mixed-state ensembles in which average symmetry can instead emerge only after averaging over microscopic trajectories. In this work, we realize decoherence-induced average SPT (ASPT) order on programmable quantum processors. Starting from a one-dimensional cluster SPT, we engineer sublattice-selective Pauli-Z dephasing through ancilla-assisted quantum circuits. We diagnose the loss of strong symmetry through the decay of the symmetry charge, while the engineered channel preserves the corresponding symmetry at the ensemble level. Moreover, a two-replica Rényi-2 string correlator measured through destructive SWAP readout remains nontrivial, revealing the ASPT structure encoded at the density-matrix level. We further show that the engineered dephasing redistributes spectral weight among reduced-stabilizer sectors while preserving the characteristic twofold pairing of the half-chain entanglement spectrum. These results establish a gate-based route to engineering and probing ASPT order and demonstrate structured decoherence as a programmable resource for realizing mixed-state topological quantum matter.

INTRODUCTION

Symmetry-protected topological (SPT) phases provide a framework for quantum matter beyond the conventional Landau-Ginzberg-Wilson symmetry breaking paradigm [1–9]. An SPT phase is short-range entangled in the bulk, but cannot be continuously deformed into a trivial product state without either closing the gap or breaking the protecting symmetry [1, 4, 6]. Its nontrivial structure is reflected in characteristic signatures including projective edge representations, degeneracies in the entanglement spectrum, and nonlocal string order [3, 4, 10–14]. These properties make SPT phases a useful setting for studying how symmetry, entanglement, and topology can be detected in experimentally accessible quantum many-body systems.

The experimental study of SPT phases has advanced rapidly with programmable quantum simulators and processors [15–21], which also enable non-unitary dynamics through post-selection and measurement [22–30]. While experiments across superconducting, trapped-ion, Rydberg, and photonic platforms have characterized SPT states through edge, string-order, and dynamical signatures [15, 17, 19, 21, 31–33], most realizations remain focused on pure or approximately coherent states. Open and noisy quantum systems instead naturally produce mixed states, for which symmetry admits distinct realizations. A strong symmetry constrains the density matrix separately under left and right symmetry actions, whereas a weak symmetry requires only invariance under conjugation [34–41]. In an ensemble representation, such a weak symmetry can arise as an average symmetry: individual trajectories need not be symmetric, provided that the ensemble is invariant under the symmetry action. This distinction enables average SPT (ASPT) phases, in which symmetry may be broken in individual trajectories but restored after ensemble averaging [36–38, 42–56]. A recent Rydberg-array experiment realized average-symmetry topology through structural disorder [57]. More recently, mixed-state SPT order and strong-to-weak symmetry breaking were probed in a five-qubit superconducting array using controlled dephasing [58]. A remaining challenge is to establish ASPT order at larger scales while directly resolving both its nonlocal order and projective edge structure at the density-matrix level.

Here, we address these challenges by realizing a decoherence-induced averaged cluster SPT at substantially larger scales on IBM quantum processors, with programmable control of the decohering ensemble and access to its mixed-state topological structure [36–38, 57–59]. Starting from a one-dimensional cluster-state SPT, we engineer local Pauli-Z dephasing on the even sublattice using ancilla qubits; the ancilla outcomes resolve individual dephasing trajectories, whose ensemble average defines the ASPT mixed state [4, 34, 60–64]. The resulting state realizes a hybrid symmetry structure in which the odd-sublattice symmetry remains strong while the even-sublattice symmetry survives only as an average symmetry [36–40, 51]. We first observe the decay of the even-sublattice symmetry charge, signaling the loss of strong symmetry, and show that the conventional single-copy string order is suppressed by trajectory-dependent sign averaging. We then probe the mixed-state ASPT order using a two-replica destructive-SWAP measurement of the normalized Rényi-2 string correlator, which remains nontrivial even when the single-copy signal is strongly suppressed [36–38]. Finally, the reconstructed

* e0554228@u.nus.edu
† xuejiayu@eitech.edu.cn
‡ phylch@nus.edu.sg

half-chain density-matrix spectrum shows that dephasing redistributes spectral weight among reduced-stabilizer sectors while preserving the characteristic twofold pairing of the projective edge degree of freedom [3, 4, 10, 11]. These measurements establish complementary symmetry, nonlinear string-order, and spectral signatures of decoherence-induced ASPT order on programmable quantum hardware.

RESULTS

Decoherence-induced average SPT order

For a pure SPT state $\rho_\psi = |\psi\rangle\langle\psi|$ in the trivial symmetry sector, a symmetry U_g acts strongly,

$$U_g \rho_\psi = \rho_\psi U_g = \rho_\psi, \qquad g \in G. \tag{1}$$

For mixed states, the symmetry can instead be realized only at the ensemble level. Writing $\rho = \sum_\eta P(\eta)|\psi_\eta\rangle\langle\psi_\eta|$, where η labels a disorder realization, decoherence trajectory, or measurement branch, the symmetry may permute individual branches as $U_g|\psi_\eta\rangle = e^{i\varphi_g(\eta)}|\psi_{g\eta}\rangle$. If $P(\eta)$ is invariant under this action, then $U_g \rho U_g^\dagger = \rho$, defining an averaged symmetry even though individual branches need not be symmetric [36–40].

We realize this structure starting from the one-dimensional cluster-state fixed point, defined by $K_j = Z_{j-1}X_jZ_{j+1}, K_j|\psi_{\rm cl}\rangle = |\psi_{\rm cl}\rangle$, and protected by $\mathbb{Z}_2^{\rm odd} \times \mathbb{Z}_2^{\rm even}$ with $U_{\rm odd/even} = \prod_{j\in{\rm odd/even}} X_j$. Its characteristic string operator,

$$\mathcal{O}_{i,k} = Z_i X_{i+1} X_{i+3} \cdots X_{k-1} Z_k, \tag{2}$$

satisfies $\langle \mathcal{O}_{i,k}\rangle = 1$ for endpoints i and k on the same sublattice [3, 10, 12, 62, 63]. For $\rho_{\rm cl} = |\psi_{\rm cl}\rangle\langle\psi_{\rm cl}|$ in the $+1$ sector, both sublattice symmetries are strong.

We convert the even-sublattice symmetry from strong to averaged by applying local Pauli-Z dephasing only on even sites,

$$\mathcal{E}_j^Z(\rho) = (1-p)\rho + pZ_j\rho Z_j, \qquad j \in \text{even}, \tag{3}$$

giving $\rho_{\rm dec} = \prod_{j\in{\rm even}} \mathcal{E}_j^Z(\rho_{\rm cl})$. The odd symmetry remains strong, $U_{\rm odd}\rho_{\rm dec} = \rho_{\rm dec}U_{\rm odd} = \rho_{\rm dec}$, whereas the even symmetry survives only under conjugation, $U_{\rm even}\rho_{\rm dec}U_{\rm even}^\dagger = \rho_{\rm dec}$. The resulting mixed state therefore realizes

$$\mathbb{Z}_2^{\rm odd,strong} \times \mathbb{Z}_2^{\rm even,average}, \tag{4}$$

as illustrated in Fig. 1 [36–38, 51]. This strong-to-average conversion defines the decoherence-induced ASPT state studied here. More generally, mixed-state SPT phases need not belong to this ASPT class (see Supplementary Material (SM)).

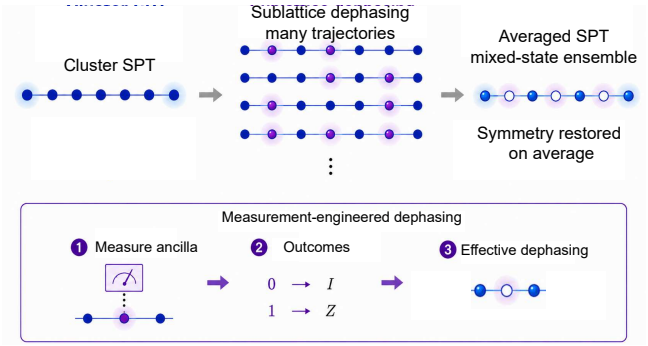

FIG. 1. Decoherence as a route to ASPT order. Starting from a pure cluster SPT with strong symmetry and protected edge/string order, local Pauli-Z dephasing engineered by measurements is applied only to the even sublattice. Each trajectory corresponds to a different probabilistic phase-flip pattern. Averaging over these trajectories yields a mixed-state ensemble with weak and average symmetry.

Quantum circuit realization and symmetry characterization

Fig. 2(a) shows the preparation circuit. Starting from $|0\rangle^{\otimes L}$, Hadamard gates and nearest-neighbor CZ gates generate

$$|\psi_{\rm cl}\rangle = \left(\prod_j {\rm CZ}_{j,j+1}\right)|+\rangle^{\otimes L}. \tag{5}$$

Pauli-Z dephasing is then engineered on each even site using an ancilla prepared as $R_y(2\theta)|0\rangle = \sqrt{1-p}\,|0\rangle + \sqrt{p}\,|1\rangle$, with $p = \sin^2\theta$, followed by a system–ancilla CZ gate. Ancilla outcomes implement I or Z_j with probabilities $1-p$ and p, respectively (see Fig. 1), so discarding the record realizes $\mathcal{E}_j^Z(\rho) = (1-p)\rho + pZ_j\rho Z_j$. Applied to all even sites, this gives

$$\rho_{\rm dec} = \sum_\eta P(\eta)\, Z(\eta)\rho_{\rm cl} Z(\eta). \tag{6}$$

Here, each ancilla record η labels a dephasing trajectory, and averaging over all records defines the ASPT mixed state [34, 36–38, 64, 65]. The corresponding IBM Quantum embedding is shown in Fig. 2 (b).

We first probe the symmetry conversion through the even-sublattice charge $Q_{\rm even} = {\rm Tr}(\rho_{\rm dec}U_{\rm even}), U_{\rm even} = \prod_{j\in{\rm even}} X_j$. Since each dephased site contributes a factor $1-2p$,

$$Q_{\rm even} = (1-2p)^{L/2}. \tag{7}$$

The measurements for $L = 20, 30$, and 40 in Fig. 2(c) follow this size-dependent decay, demonstrating the loss of strong even-sublattice symmetry. Nevertheless, $U_{\rm even}\rho_{\rm dec}U_{\rm even}^\dagger = \rho_{\rm dec}$ remains satisfied, so the even symmetry survives in the averaged sense, while the odd symmetry remains strong.

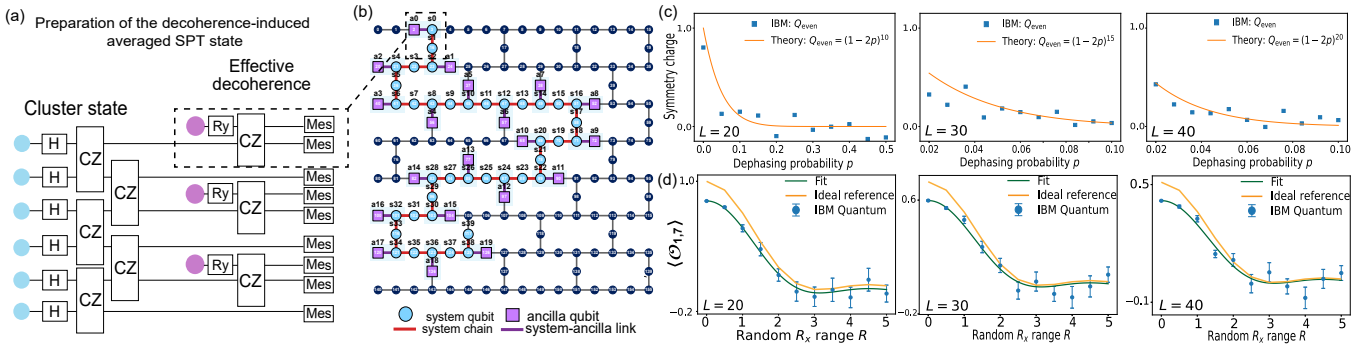

FIG. 2. **Circuit realization and hardware characterization of the decoherence-induced ASPT state. (a)** Preparation circuit: a one-dimensional cluster state is generated by Hadamard and nearest-neighbor CZ gates, followed by ancilla-assisted Pauli-Z dephasing on the even sublattice; ancilla outcomes resolve individual dephasing trajectories. **(b)** IBM Quantum embedding. Cyan and purple sites denote system and ancilla qubits, with red and purple links indicating system and system–ancilla couplings, respectively. **(c)** Even-sublattice symmetry charge $Q_{\rm even}$ versus dephasing probability p for $L = 20, 30$, and 40. IBM Quantum data (blue) follow the ideal prediction $Q_{\rm even} = (1-2p)^{L/2}$ (orange, Eq.7), showing the loss of strong even-sublattice symmetry with increasing p and L. **(d)** Single-copy string correlator $\langle \mathcal{O}_{1,7} \rangle$ [Eq. 2] versus random-rotation range R for $L = 12$ and $p = 0, 0.05$, and 0.10. IBM data (blue), ideal predictions (orange), and fits (green) show increasing suppression with R and p, illustrating the fragility of the conventional string signal under trajectory averaging and engineered decoherence.

We next examine the conventional cluster string, which under dephasing obeys

$$\langle \mathcal{O}_{i,k} \rangle_{\rm dec} = (1-2p)^{N_{\rm dep}(i,k)}, \tag{8}$$

with $N_{\rm dep}(i,k)$ the number of dephased sites on its X support. This decay results from cancellation of trajectory-dependent string signs and therefore does not imply loss of ASPT order [36–40]. To separate this controlled suppression from hardware noise, we additionally apply symmetry-preserving random rotations $U_R(\boldsymbol{\phi}) = \prod_j R_x(\phi_j)$, with independently sampled $\phi_j \sim [0, R]$. Since the interior X operators are invariant under R_x, while the two endpoint Z operators each contribute a factor $\cos\phi$, averaging over the random angles gives $\overline{\cos\phi} = \frac{1}{R}\int_0^R d\phi \cos\phi = \frac{\sin R}{R}$. The random-rotation-averaged ideal string signal therefore becomes

$$\overline{\langle \mathcal{O}_{i,k} \rangle}_{\rm ideal} = (\frac{\sin R}{R})^2 (1-2p)^{N_{\rm dep}(i,k)}. \tag{9}$$

As shown in Fig. 2(d), the measured string correlator follows the predicted suppression with increasing R and p, consistent with the expected effects of the programmed perturbations and engineered dephasing. This controlled suppression also illustrates the limitation of the single-copy string diagnostic, motivating the two-replica Rényi-2 probe introduced next.

Probing average SPT order with a two-replica string correlator

The central technical challenge is to recover topological information that is lost under the linear ensemble average of conventional single-copy observables. We overcome this by mapping a nonlinear density-matrix correlator onto a directly measurable two-replica observable on quantum hardware. We therefore measure the normalized Rényi-2 string correlator

$$C^{(2)}_{i,k} = \frac{{\rm Tr}(\rho_{\rm dec}\mathcal{O}_{i,k}\rho_{\rm dec}\mathcal{O}_{i,k})}{{\rm Tr}(\rho^2_{\rm dec})} \equiv \frac{N_{i,k}}{D}, \tag{10}$$

which probes the density-matrix structure of the ASPT state [36–40] (see SM for more details). Experimentally, this requires two independently prepared decohered replicas, allowing the mixed-state string order to be measured directly.

As shown in Fig. 3(a,b), two independent copies $\rho^{A,B}_{\rm dec}$ are prepared and measured using pairwise destructive SWAP readout. The denominator $D = {\rm Tr}(\rho^2_{\rm dec})$ is obtained from the global SWAP expectation, while the numerator $N_{i,k}$ uses the same circuit with $\mathcal{O}_{i,k}$ inserted on replica A before readout (see SM for details).

The robustness of this diagnostic follows from the dephasing trajectories $|\psi_{\boldsymbol{\eta}}\rangle = Z(\boldsymbol{\eta})|\psi_{\rm cl}\rangle$, for which $\mathcal{O}_{i,k}|\psi_{\boldsymbol{\eta}}\rangle = s_{\boldsymbol{\eta}}|\psi_{\boldsymbol{\eta}}\rangle$ with $s_{\boldsymbol{\eta}} = \pm 1$. While the single-copy correlator averages $s_{\boldsymbol{\eta}}$ and can vanish by cancellation, the doubled correlator depends on $s^2_{\boldsymbol{\eta}} = 1$; for orthogonal dephasing sectors,

$$C^{(2)}_{i,k,{\rm ideal}} = \frac{\sum_{\boldsymbol{\eta}} P(\boldsymbol{\eta})^2 s^2_{\boldsymbol{\eta}}}{\sum_{\boldsymbol{\eta}} P(\boldsymbol{\eta})^2} = 1. \tag{11}$$

Figs. 3(c,d) compare the two diagnostics for $L = 6$. The single-copy signal decays as $(1-2p)^2$, whereas the measured $C^{(2)}_{i,k}$ remains weakly dependent on p and close to the ideal value 1. This response is a key experimental signature: trajectory averaging suppresses the conventional string signal, while the nonlinear Rényi-2 correlator recovers the topological information encoded in the

mixed-state density matrix. At $p = 0.1$, Fig. 3(e) further shows a clearly resolvable doubled-string signal for $L = 8$ and 12, demonstrating that this nonlinear mixed-state diagnostic remains accessible beyond the minimal system size on current quantum hardware (see SM for more details).

Persistence of the entanglement-spectrum degeneracy

The doubled-string correlator reveals hidden nonlocal order, but an independent question is whether the projective edge structure inherited from the parent SPT survives ensemble averaging. We therefore reconstruct the half-chain reduced density matrix of an $L = 8$ cluster chain using quantum state tomography from repeated single-copy measurements. For $\rho_A = \mathrm{Tr}_{\bar{A}}\,\rho$, we define the spectral levels $\xi_\alpha = -\log \lambda_\alpha$, where λ_α are the eigenvalues of ρ_A [3, 4, 10, 11, 62, 63, 66–69].

For the cluster fixed point, the spectrum exhibits the characteristic twofold degeneracy associated with the projective SPT edge degree of freedom. Each dephasing trajectory, $|\psi_{\boldsymbol{\eta}}\rangle = Z(\boldsymbol{\eta})|\psi_{\mathrm{cl}}\rangle$, preserves this pairing because across the bipartition $Z(\boldsymbol{\eta}) = Z_A(\boldsymbol{\eta}_A) \otimes Z_{\bar{A}}(\boldsymbol{\eta}_{\bar{A}})$ acts only by local unitaries and therefore leaves the Schmidt values unchanged. After discarding the trajectory record,

$$\rho_A^{\mathrm{dec}} = \sum_{\boldsymbol{\eta}_A} P_A(\boldsymbol{\eta}_A) Z_A(\boldsymbol{\eta}_A) \rho_A^{\mathrm{cl}} Z_A(\boldsymbol{\eta}_A), \tag{12}$$

so dephasing redistributes weight among reduced-stabilizer sectors without resolving the edge doublet. Equivalently, we have

$$\rho_A^{\mathrm{dec}} = \sum_{\mu} w_\mu\, \rho_{A,\mathrm{bulk}}^{(\mu)} \otimes \frac{\mathbb{I}_{\mathrm{edge}}}{2}, \tag{13}$$

where μ labels the dephasing-induced bulk sectors [36–40]. Thus, dephasing changes the spectral weights while preserving the characteristic twofold edge pairing.

Fig. 4 compares the measured spectra with the ideal predictions. At $p = 0$, the ideal half-chain reduced state has $\lambda_{1,2} = 1/2$, corresponding to $\xi_{1,2} = \ln 2$, and the experiment reproduces the leading twofold degeneracy. At $p = 0.1$, dephasing populates an additional stabilizer-syndrome sector, yielding ideally $\lambda_{1,2} = 0.45$ and $\lambda_{3,4} = 0.05$ ($\xi_{1,2} \simeq 0.799$ and $\xi_{3,4} \simeq 2.996$, see SM for more details). The measured spectrum follows this paired structure: the dominant levels remain nearly degenerate while a higher-lying pair emerges at the expected scale. Small deviations are most visible in the weakly populated higher sector, which is more sensitive to sampling and hardware errors. The preserved pairwise organization therefore provides a complementary signature that engineered dephasing redistributes bulk-sector weight without lifting the SPT edge degeneracy.

DISCUSSION

In this work, we realize a decoherence-induced average SPT state on programmable quantum processors by engineering sublattice-selective Pauli-Z dephasing of a one-dimensional cluster SPT. The resulting channel converts the even-sublattice symmetry from a strong symmetry to an average symmetry while leaving the odd-sublattice symmetry strong. Our measurements reveal that the symmetry charge and conventional single-copy string correlator decay under dephasing, whereas the two-replica Rényi-2 string correlator, defined at the density-matrix level, remains nontrivial. Moreover, the reconstructed half-chain spectrum further shows that dephasing redistributes spectral weight among reduced-stabilizer sectors while preserving the characteristic twofold pairing.

Our results establish engineered decoherence as a controllable route to mixed-state topological order on gate-based quantum hardware. More broadly, this framework can be extended to two-dimensional cluster SPT states exhibiting decoherence-driven topological transitions [70], interacting SPT states away from the exactly solvable cluster limit [52], and intrinsically mixed-state topological phases generated from topologically ordered states such as the toric code [71, 72]. Spatially correlated decoherence provides another natural direction for exploring how the structure of the environment controls the stability and transition of mixed-state topological order [73].

ACKNOWLEDGEMENTS

We acknowledge the use of IBM Quantum services for this work. The views expressed are those of the authors and do not reflect the official policy or position of IBM or the IBM Quantum team. This work is supported by the Singapore Ministry of Education Academic Research Fund Tier-II Grant (MOE-T2EP50224-0007). X.-J. Yu was supported by the National Natural Science Foundation of China (Grant No.12405034) and a start-up grant from Eastern Institute of Technology, Ningbo.

DATA AND CODE AVAILABILITY

All data and code for this work are available from the corresponding authors upon reasonable request.

AUTHOR CONTRIBUTIONS.

R.S. conceived the project, designed and performed the quantum-hardware experiments, carried out the numerical simulations, analyzed the results, and wrote the manuscript. X.-J.Y. contributed to the theoretical analysis and interpretation of the results. C.H.L. supervised

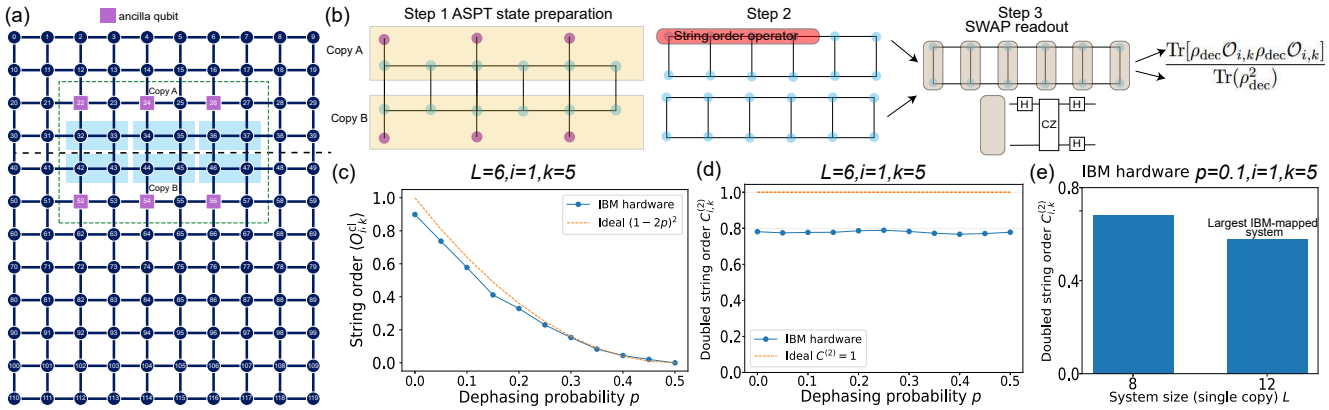

FIG. 3. **Two-replica measurement of the Rényi-2 string diagnostic of ASPT order.** **(a)** Hardware embedding of two independently dephased replicas A and B. **(b)** Protocol for $C^{(2)}_{i,k}$ [Eq. 10]: two copies of $\rho_{\rm dec}$ are prepared [see the setup shown in Fig. 2 (a) for each copy], $\mathcal{O}_{i,k}$ is inserted only for the numerator, and pairwise destructive-SWAP readout yields $N_{i,k} = \mathrm{Tr}(\rho_{\rm dec}\mathcal{O}_{i,k}\rho_{\rm dec}\mathcal{O}_{i,k})$ and $D = \mathrm{Tr}(\rho^2_{\rm dec})$, with $C^{(2)}_{i,k} = N_{i,k}/D$. **(c,d)** Single-copy $\langle\mathcal{O}_{i,k}\rangle$ [Eq. 2] and doubled $C^{(2)}_{i,k}$ [Eq. 10] versus dephasing probability p for $L = 6$. The single-copy signal decays with p, whereas $C^{(2)}_{i,k}$ remains approximately independent of p and clearly nonzero, despite a hardware-induced reduction from the ideal value 1. At $p = 0$, retaining the system–ancilla CZ layer produces a residual hardware-induced reduction from unity. **(e)** Measured $C^{(2)}_{i,k}$ at $p = 0.1$ for $L = 8$ and 12, showing a robust doubled-string signal up to the largest system implemented.

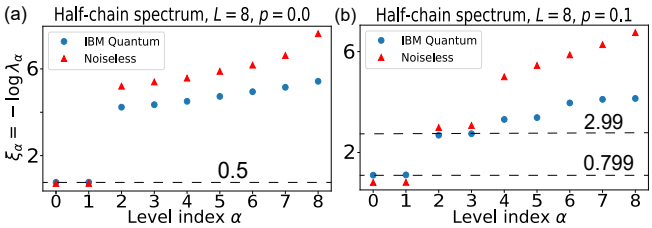

FIG. 4. **Measurements of half-chain entanglement spectrum from density-matrix reconstruction on quantum hardware.** For an $L = 8$ chain (single copy), the reduced density matrix ρ_A is obtained by tracing out half of the system, with entanglement levels $\xi_\alpha = -\log\lambda_\alpha$. Blue circles denote IBM Quantum data and red triangles the noiseless reference. (a) At $p = 0$, the two lowest levels exhibit the characteristic near-degenerate pair associated with the cluster-state edge sector. (b) At $p = 0.1$, dephasing redistributes spectral weight into an additional reduced-stabilizer sector while preserving the pairwise structure. Dashed lines mark the ideal values $\xi_{1,2} \simeq 0.799$ and $\xi_{3,4} \simeq 2.996$. Larger deviations in the higher levels reflect their smaller spectral weight and greater sensitivity to sampling and hardware errors. See Supplementary Material for more details.

the project. All authors discussed the results and approved the final manuscript.

[1] X. Chen, Z.-C. Gu, and X.-G. Wen, Complete classification of one-dimensional gapped quantum phases in interacting spin systems, Physical Review B **84**, 235128 (2011).

[2] Y.-Z. You and C. Xu, Symmetry-protected topological states of interacting fermions and bosons, Physical Review B **90**, 245120 (2014), arXiv:1409.0168 [cond-mat.str-el].

[3] F. Pollmann, A. M. Turner, E. Berg, and M. Oshikawa, Entanglement spectrum of a topological phase in one dimension, Physical Review B **81**, 064439 (2010).

[4] F. Pollmann, E. Berg, A. M. Turner, and M. Oshikawa, Symmetry protection of topological phases in one-dimensional quantum spin systems, Physical Review B **85**, 075125 (2012).

[5] R. Morral-Yepes, F. Pollmann, and I. Lovas, Detecting and stabilizing measurement-induced symmetry-

protected topological phases in generalized cluster models, Phys. Rev. B **108**, 224304 (2023), arXiv:2302.14551 [cond-mat.stat-mech].

[6] X. Chen, Z.-C. Gu, Z.-X. Liu, and X.-G. Wen, Symmetry protected topological orders and the group cohomology of their symmetry group, Physical Review B **87**, 155114 (2013), arXiv:1106.4772 [cond-mat.str-el].

[7] C. Zhang, Y. Xu, J.-H. Zhang, C. Xu, Z. Bi, and Z.-X. Luo, Strong-to-weak spontaneous breaking of 1-form symmetry and intrinsically mixed topological order, Phys. Rev. B **111**, 115137 (2025), arXiv:2409.17530 [quant-ph].

[8] X.-J. Yu, L. Xu, and H.-Q. Lin, Topological physics in quantum critical systems, Physics Reports **1160**, 1 (2026).

[9] L. H. Santos, J. Cano, M. Mulligan, and T. L. Hughes, Symmetry-protected topological interfaces and entanglement sequences, Phys. Rev. B **98**, 075131 (2018), arXiv:1803.04418.

[10] F. Pollmann and A. M. Turner, Detection of symmetry-protected topological phases in one dimension, Physical Review B **86**, 125441 (2012).

[11] H. Li and F. D. M. Haldane, Entanglement spectrum as a generalization of entanglement entropy: Identification of topological order in non-abelian fractional quantum hall effect states, Physical Review Letters **101**, 010504 (2008), arXiv:0805.0332 [cond-mat.mes-hall].

[12] T. Kennedy and H. Tasaki, Hidden symmetry breaking and the haldane phase in $S = 1$ quantum spin chains, Communications in Mathematical Physics **147**, 431 (1992).

[13] Y.-Z. You, Z. Bi, A. Rasmussen, K. Slagle, and C. Xu, Wave function and strange correlator of short-range entangled states, Phys. Rev. Lett. **112**, 247202 (2014), arXiv:1312.0626.

[14] S. Matsuura, X. Wen, L.-Y. Hung, and S. Ryu, Charged topological entanglement entropy, Phys. Rev. B **93**, 195113 (2016), arXiv:1601.03751.

[15] S. de Léséleuc, V. Lienhard, P. Scholl, D. Barredo, S. Weber, N. Lang, H. P. Büchler, T. Lahaye, and A. Browaeys, Experimental realization of a symmetry protected topological phase of interacting bosons with rydberg atoms, Science **365**, 775 (2019), arXiv:1810.13286 [quant-ph].

[16] A. T. K. Tan, S.-N. Sun, R. N. Tazhigulov, G. K.-L. Chan, and A. J. Minnich, Realizing symmetry-protected topological phases in a spin-1/2 chain with next-nearest-neighbor hopping on superconducting qubits, Phys. Rev. A **107**, 032614 (2023), arXiv:2112.10333 [quant-ph].

[17] X. Zhang, W. Jiang, J. Deng, K. Wang, J. Chen, P. Zhang, W. Ren, H. Dong, S. Xu, Y. Gao, F. Jin, X. Zhu, Q. Guo, H. Li, C. Song, A. V. Gorshkov, T. Iadecola, F. Liu, Z.-X. Gong, Z. Wang, D.-L. Deng, and H. Wang, Digital quantum simulation of floquet symmetry-protected topological phases, Nature **607**, 468 (2022).

[18] R. Verresen, R. Moessner, and F. Pollmann, One-dimensional symmetry protected topological phases and their transitions, Phys. Rev. B **96**, 165124 (2017), arXiv:1707.05787 [cond-mat.str-el].

[19] P. T. Dumitrescu, J. G. Bohnet, J. P. Gaebler, A. Hankin, D. Hayes, A. Kumar, B. Neyenhuis, R. Vasseur, and A. C. Potter, Dynamical topological phase realized in a trapped-ion quantum simulator, Nature **607**, 463 (2022).

[20] R. Shen, T. Chen, B. Yang, Y. Zhong, and C. H. Lee, Robust simulations of many-body symmetry-protected topological phase transitions on a quantum processor, npj Quantum Information **11**, 179 (2025), arXiv:2503.08776 [quant-ph].

[21] G. Pennington, K. C. Smith, J. R. Garrison, L. P. Lindoy, J. Crain, and B. Jaderberg, Preparing 100-qubit symmetry-protected topological order on a digital quantum computer, arXiv preprint arXiv:2603.06325 (2026).

[22] Google Quantum AI and Collaborators, Measurement-induced entanglement and teleportation on a noisy quantum processor, Nature **622**, 481 (2023).

[23] T. Chen, R. Shen, C. H. Lee, and B. Yang, High-fidelity realization of the aklt state on a nisq-era quantum processor, SciPost Physics **15**, 170 (2023).

[24] K. C. Smith, E. Crane, N. Wiebe, and S. Girvin, Deterministic constant-depth preparation of the aklt state on a quantum processor using fusion measurements, PRX Quantum **4**, 020315 (2023).

[25] J. M. Koh, S.-N. Sun, M. Motta, and A. J. Minnich, Measurement-induced entanglement phase transition on a superconducting quantum processor with mid-circuit readout, Nature Physics **19**, 1314 (2023).

[26] K. Su, N. Myerson-Jain, and C. Xu, Conformal field theories generated by chern insulators under decoherence or measurement, Phys. Rev. B **109**, 035146 (2024).

[27] J. M. Koh, W.-T. Xue, T. Tai, D. E. Koh, and C. H. Lee, Interacting non-hermitian edge and cluster bursts on a digital quantum processor, Nature Communications **17**, 9120 (2026).

[28] C. Xu, C. H. Lee, H.-H. Tu, and Y. Zhang, A fractional quantum hall factory on quantum processors: constant-depth preparation of clustered non-abelian states, arXiv preprint arXiv:2608.05140 (2026).

[29] T.-C. Lu, L. A. Lessa, I. H. Kim, and T. H. Hsieh, Measurement as a shortcut to long-range entangled quantum matter, PRX Quantum **3**, 040337 (2022), arXiv:2206.13527.

[30] K. Su, N. Myerson-Jain, C. Wang, C.-M. Jian, and C. Xu, Higher-form symmetries under weak measurement, Phys. Rev. Lett. **132**, 200402 (2024), arXiv:2304.14433 [cond-mat.str-el].

[31] M. Iqbal, N. Tantivasadakarn, R. Verresen, S. L. Campbell, J. M. Dreiling, C. Figgatt, J. P. Gaebler, J. Johansen, M. Mills, S. A. Moses, J. M. Pino, A. Ransford, M. Rowe, P. Siegfried, R. P. Stutz, M. Foss-Feig, A. Vishwanath, and H. Dreyer, Non-abelian topological order and anyons on a trapped-ion processor, Nature **626**, 505 (2024).

[32] N. Tantivasadakarn, R. Thorngren, A. Vishwanath, and R. Verresen, Long-range entanglement from measuring symmetry-protected topological phases, Physical Review X **14**, 021040 (2024), arXiv:2112.01519 [cond-mat.str-el].

[33] N. Sadoune, I. Pogorelov, C. L. Edmunds, G. Giudici, G. Giudice, C. D. Marciniak, M. Ringbauer, T. Monz, and L. Pollet, Learning symmetry-protected topological order from trapped-ion experiments, Quantum **10**, 2100 (2026), arXiv:2408.05017 [quant-ph].

[34] M. A. Nielsen and I. L. Chuang, *Quantum Computation and Quantum Information: 10th Anniversary Edition* (Cambridge University Press, Cambridge, 2010).

[35] M. M. Wilde, *Quantum Information Theory*, 2nd ed. (Cambridge University Press, Cambridge, 2017) arXiv:1106.1445 [quant-ph].

[36] R. Ma and C. Wang, Average symmetry-protected topological phases, Physical Review X **13**, 031016 (2023), arXiv:2209.02723 [cond-mat.str-el].

[37] R. Ma, J.-H. Zhang, Z. Bi, M. Cheng, and C. Wang, Topological phases with average symmetries: The decohered, the disordered, and the intrinsic, Physical Review X **15**, 021062 (2025), arXiv:2305.16399 [cond-mat.str-el].

[38] R. Ma and A. Turzillo, Symmetry-protected topological phases of mixed states in the doubled space, PRX Quantum **6**, 010348 (2025), arXiv:2403.13280 [quant-ph].

[39] H. Xue, J. Y. Lee, and Y. Bao, Tensor network formulation of symmetry protected topological phases in mixed states, arXiv preprint arXiv:2403.17069 (2024).

[40] Y. Guo, J.-H. Zhang, H.-R. Zhang, S. Yang, and Z. Bi, Locally purified density operators for symmetry-protected topological phases in mixed states, Physical Review X **15**, 021060 (2025).

[41] Y. Guo, S. Yang, and X.-J. Yu, Quantum strong-to-weak spontaneous symmetry breaking in decohered one-dimensional critical states, PRX Quantum **6**, 040311 (2025).

[42] S. Sang, L. A. Lessa, R. S. K. Mong, T. Grover, C. Wang, and T. H. Hsieh, Mixed-state phases from local reversibility, Physical Review X 10.1103/1kr5-jlcb (2026), accepted 19 August 2026.

[43] N. Manjunath, A. Turzillo, and C. Wang, Detection of 2d SPT phases under decoherence, (2025), arXiv:2507.00127 [cond-mat.str-el].

[44] S. Sun, J.-H. Zhang, Z. Bi, and Y. You, Holographic view of mixed-state symmetry-protected topological phases in open quantum systems, PRX Quantum **6**, 020333 (2025).

[45] R. Luo, Y.-N. Wang, and Z. Bi, Topological holography for mixed-state phases and phase transitions, PRX Quantum **6**, 040358 (2025), arXiv:2507.06218 [quant-ph].

[46] T. D. Ellison and M. Cheng, Toward a classification of mixed-state topological orders in two dimensions, PRX Quantum **6**, 010315 (2025).

[47] Y.-H. Chen and T. Grover, Separability transitions in topological states induced by local decoherence, Physical Review Letters **132**, 170602 (2024).

[48] Y. Bao, R. Fan, A. Vishwanath, and E. Altman, Mixed-state topological order and the errorfield double formulation of decoherence-induced transitions, Physical Review Letters **136**, 220402 (2026).

[49] A. Moharramipour, L. A. Lessa, C. Wang, T. H. Hsieh, and S. Sahu, Symmetry-enforced entanglement in maximally mixed states, PRX Quantum **5**, 040336 (2024).

[50] R. Fan, Y. Bao, E. Altman, and A. Vishwanath, Diagnostics of mixed-state topological order and breakdown of quantum memory, PRX Quantum **5**, 020343 (2024).

[51] Z. Zhang, U. Agrawal, and S. Vijay, Quantum communication and mixed-state order in decohered symmetry-protected topological states, Physical Review B **111**, 115141 (2025), arXiv:2405.05965 [quant-ph].

[52] J. Y. Lee, Y.-Z. You, and C. Xu, Symmetry protected topological phases under decoherence, Quantum **9**, 1607 (2025), arXiv:2210.16323.

[53] L. A. Lessa, M. Cheng, and C. Wang, Mixed-state quantum anomaly and multipartite entanglement, Physical Review X **15**, 011069 (2025).

[54] S. Lu, L. Q. Silveira, and Y. You, Nonequilibrium topological response under charge dephasing, arXiv preprint arXiv:2602.23484 (2026).

[55] L. Li, Z. Bi, and W. Cao, Generalized symmetry-protected topological phases in mixed states from gauging dualities, arXiv preprint arXiv:2603.17282 (2026).

[56] L. A. Lessa, R. Ma, J.-H. Zhang, Z. Bi, M. Cheng, and C. Wang, Strong-to-weak spontaneous symmetry breaking in mixed quantum states, PRX Quantum **6**, 010344 (2025), arXiv:2405.03639.

[57] Z. Yue, Y.-F. Mao, X. Liang, Z.-X. Hua, P. Ge, Y.-X. Chao, K. Li, C. Jia, M. K. Tey, Y. Xu, and L. You, Average topological phase in a disordered rydberg atom array, Nature Physics **22**, 844 (2026).

[58] Q. Cao, Z. Bi, and K. W. Murch, Mixed-state symmetry-protected topology and strong-to-weak spontaneous symmetry breaking in a superconducting qubit array (2026), arXiv:2608.24993 [quant-ph].

[59] Y. Zhang, T. H. Hsieh, Y. B. Kim, and Y. Zou, Probing mixed-state phases on a quantum computer via Renyi correlators and variational decoding, Nature Communications **17**, 8047 (2026), arXiv:2505.02900.

[60] R. Raussendorf and H. J. Briegel, A one-way quantum computer, Physical Review Letters **86**, 5188 (2001), arXiv:quant-ph/0010033.

[61] M. Hein, J. Eisert, and H. J. Briegel, Multi-party entanglement in graph states, Physical Review A **69**, 062311 (2004), arXiv:quant-ph/0307130.

[62] W. Son, L. Amico, and V. Vedral, Topological order in 1d cluster state protected by symmetry, Quantum Information Processing **11**, 1961 (2012), arXiv:1111.7173 [quant-ph].

[63] D. V. Else, I. Schwarz, S. D. Bartlett, and A. C. Doherty, Symmetry-protected phases for measurement-based quantum computation, Phys. Rev. Lett. **108**, 240505 (2012), arXiv:1201.4877 [quant-ph].

[64] K. Kraus, *States, Effects, and Operations: Fundamental Notions of Quantum Theory*, Lecture Notes in Physics, Vol. 190 (Springer, Berlin, Heidelberg, 1983).

[65] N. Myerson-Jain, T. L. Hughes, and C. Xu, Decoherence through ancilla anyon reservoirs, Phys. Rev. Lett. **134**, 096503 (2025), arXiv:2312.04638 [cond-mat.str-el].

[66] O. E. Sommer, X. Wen, and A. Vishwanath, Higher berry curvature from the wave function. i. schmidt decomposition and matrix product states, Phys. Rev. Lett. **134**, 146601 (2025), arXiv:2405.05316 [cond-mat.str-el].

[67] X.-J. Yu, S. Yang, H.-Q. Lin, and S.-K. Jian, Universal entanglement spectrum in one-dimensional gapless symmetry protected topological states, Phys. Rev. Lett. **133**, 026601 (2024).

[68] W.-H. Zhong, H.-Q. Lin, and X.-J. Yu, Quantum entanglement of fermionic symmetry-enriched quantum critical points in one dimension, Phys. Rev. B **112**, 075129 (2025).

[69] Y. Guo, S. Yang, and X.-J. Yu, Generalized li-haldane correspondence in critical free-fermion systems, Phys. Rev. Res. **8**, 023203 (2026).

[70] Y. Guo and Y. Ashida, Two-dimensional symmetry-protected topological phases and transitions in open quantum systems, Physical Review B **109**, 195420 (2024), arXiv:2311.12619 [quant-ph].

[71] Z. Wang, Z. Wu, and Z. Wang, Intrinsic mixed-state topological order, PRX Quantum **6**, 010314 (2025), arXiv:2307.13758 [cond-mat.str-el].

[72] S. Sang, Y. Zou, and T. H. Hsieh, Mixed-state quantum phases: Renormalization and quantum error correction, Physical Review X **14**, 031044 (2024), arXiv:2310.08639

[quant-ph].
[73] S. Chirame, F. J. Burnell, S. Gopalakrishnan, and A. Prem, Stable symmetry-protected topological phases in systems with heralded noise, Physical Review Letters **134**, 010403 (2025), arXiv:2404.16962 [quant-ph].

Supplementary Files

This is a list of supplementary files associated with this preprint. Click to download.

- RuizheASPTsupp.pdf